Moroccan Journal of Chemistry
ISSN: 2351-812X
http://revues.imist.ma/?journal=morjchem&page=login
ELGhayati & al. / Mor. J. Chem. 7 N°3 (2019) 567-579

Experimental and theoretical investigation of 4-Methyl-2,3-dihydro-1H-1,5-benzodiazepin-2-one on the corrosion and inhibition behavior of steel in acidic solution

L. El Ghayati[1], A. Batah[2], M. Belkhaouda[2,3], L. Bammou[2], R. Salghi[2], A. Saber[1], A. Chetouani[4] M. L. Taha[5], E. M. Essassi[1]

[1]Laboratoire de Chimie Organique Hétérocyclique, Centre de Recherche des Sciences des Médicaments, Pôle de Compétences Pharmacochimie, Mohammed V University in Rabat, Faculté des Sciences, Av. Ibn Battouta, BP 1014 Rabat, Morocco,

[2]Laboratory of Environmental Engineering and Biotechnology, ENSA, Ibn Zohr University, PO Box 1136, 80000 Agadir, Morocco

[3]Laboratoire de chimie physique, Centre Régionale des Métiers de l'Education et de Formation Sous Massa, Inzegane, Morocco

4 Laboratoire de Chimie physique; Centre Régionale des Métiers de l'Education et de Formation Oujda, Morocco.

[5] Laboratoire de Chimie Bioorganique Appliquee , Faculte´ des sciences, Universite´ Ibn Zohr, Agadir.

* *Corresponding author:*
bammou@yahoo.fr

Received 23 Dec 2018,
Revised 15 April 2019,
Accepted 06 Aug 2019

Abstract

The effect of 4-methyl-2,3-dihydro-1H-1,5-benzodiazepin-2-one (**MDBO**) on the inhibition of steel corrosion was studied in an acid medium. This inhibiting action against corrosion of steel in a corrosive solution was studied at 298 K using potentiodynamic polarization curves, weight loss measurements and electrochemical impedance spectroscopy (EIS) and complementary with density functional theory (DFT) methods. The inhibiting action increases with the concentration of (**MDBO**) compound to attain 89.53% at 10^{-3} M. Polarization measurements also show that the 4-methyl-2,3-dihydro-1H-1,5-benzodiazepin-2-one (**MDBO**) acts essentially as a mixte type inhibitor. The cathodic curves indicate that the reduction of proton at the steel surface happens with an activating mechanism. (**MDBO**) adsorbs on the steel surface according to Langmuir adsorption model. Effect of temperature is also made in the 298–328 K range. Activation parameters are determined and discussed. For establish the correlation between experimental data and theoretical results, some quantum chemical parameters for the tested compound were evaluated for supply more idea on the mechanism of inhibition of the dissolution process..

Keywords: *Polarization, Carbon Steel, Inhibition, Acid medium, Corrosion.*

1. Introduction

Steel with its relatively high strength, low cost, and widespread availability has been extensively utilized in numerous industrial applications such as petrochemical plants, power plants, oil and gas refineries, distillers, and ships[1-3]. Corrosion of metals is a major problem that must be confronted for safety, environment, and economic reasons. It can be minimized by suitable strategies which in turn stifle, retard or completely stop the cathodic or anodic reactions or both [4]. Among the several methods of corrosion control and prevention, the use of corrosion inhibitors, is very popular. Corrosion inhibitors efficiently reduce the undesirable destructive effect and prevent metal dissolution. The use of inhibitors for the control of corrosion of metals and alloys, which are in contact with the aggressive environment, is therefore essential. The role of inhibitors added in low concentrations to corrosive media is to decrease the dissolution of the metal with corrosive medium and is to inhibit the adsorption or coordination onto the metal surfaces [5–12]. Organic compounds bearing heteroatoms with high electron density such as phosphorous, sulfur, nitrogen, oxygen or those containing multiple bonds which are considered as adsorption centers, are effective as the corrosion inhibitor [13–14]. In general, the adsorption of an inhibitor on a metal surface depends on the nature, its chemical structure, the surface charge of the metal, the adsorption mode and the type of electrolyte solution. The present work continues to focus on the application of organic compound 4-methyl-2,3-dihydro-1H-1,5-benzodiazepin-2-one (**MDBO**) (Fig. 1) for metallic corrosion control and reports their inhibiting effects for carbon steel corrosion in acidic solution at different concentration and temperature using potentiodynamic polarization, impedance spectroscopy (EIS) methods and weight loss, studied by weight loss measurements.

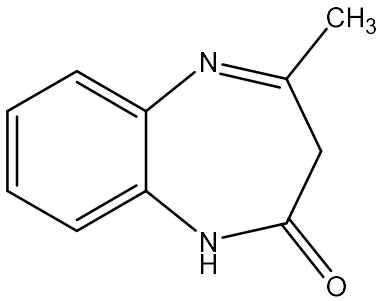

Figure 1. Structure of 4-methyl-2,3-dihydro-1H-1,5-benzodiazepin-2-one (**MDBO**)

1. Methods and materials

1.1 Synthesis of inhibitors

The *o*-Phenylenediamine (9 mmol) and ethyl acetoacetate (9 mmol) were heated in xylene (10 ml) for 1 hour. The mixture was set aside for the growth of colorless crystals of 4-methyl-2,3-dihydro-1H-1,5-benzodiazepin-2-one.

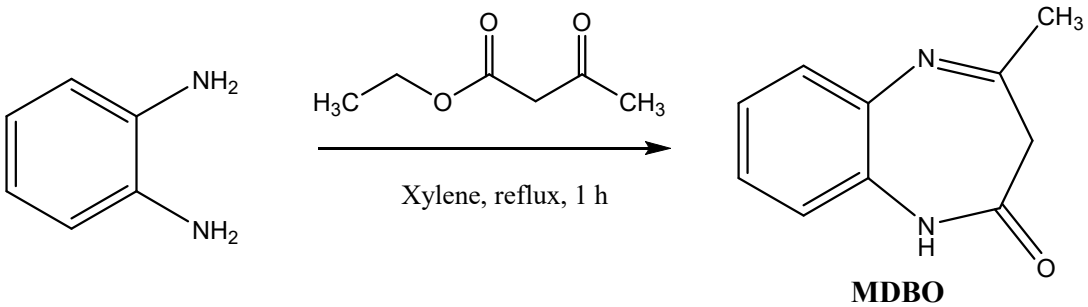

Scheme 2: Synthesis of 4-methyl-2,3-dihydro-1H-1,5-benzodiazepin-2-one: (**MDBO**).

The analytical and spectroscopic data are conforming to the structure of compound formed. **Yield** = 88%; **M.p**.449–451**K**; ^{1}**H NMR (CDCl$_3$) δ ppm**: 2.38 (s, 3H, CH_3); 3.59 (s, 2H, CH_2); 7.08–7.37 (m, 4H); 9.35 (s, 1H, NH). ^{13}**C NMR (CDCl$_3$) δ ppm**: 28.01 (CH_3); 43.57 (CH_2); 121.88–139.62 (Car); 162.89 (CN); 167.36 (CO). Thus crystallographic study by X-ray diffraction was performed to verify the exact structure of the compound (**MDBO**) [15-16].

1.2. Electrolyte and work electrode

The aggressive solution, 1.0 M HCl were prepared by dilution of an analytical grade 37% HCl with distilled water. The concentration range of inhibitor employed was 10^{-3} to 10^{-6} mol /L. The chemical composition of the working electrode, a carbon steel electrode, is given in Table 1.

Table 1: Chemical composition of steel specimens.

Elements	**Fe**	**C**	**Si**	**Mn**	**Cu**	**S**	**Cr**	**Co**	**Ti**	**Ni**
Mass %	98.307	0.38	0.23	0.68	0.16	0.016	0.077	0.09	0.011	0.059

The samples were polished mechanically with different grades (600, 800, and 1200) silicon carbide paper, degreased in acetone, washed with distilled water and dried in warm prior to each use.

2. Experimental

2.1. Weight loss measurement:

Gravimetric measurements were carried out in a double walled glass cell equipped with a thermostated cooling condenser. The solution volume was 100 ml. The steel specimens used had a rectangular form (2 x 2 x 0.08 cm^3) immersed in acid solution 1M HCl for 6 hours. All solutions were prepared with bidistilled water. The experiments were performed in aerated solutions at 298K using a thermostatic bath.

2.2. Electrochemical measurements

2.2.1. Potentiodynamique Polarization curves

The electrochemical behavior of carbon steel sample in inhibited and solution containing different concentrations of the tested inhibitor was carried out using a potentiostat PGZ100 operated by Voltamaster software. This device is connected to a cell with three electrode thermostats with double wall (Tacussel Standard CEC/TH). A saturated calomel electrode (SCE) and platinum electrode were used as reference and auxiliary electrodes, respectively. The same material used for gravimetric measurements form the working electrode. The surface area exposed to the electrolyte is 0.32 cm^2. Potentiodynamic polarization curves, obtained from −800 mV to −200 mV/SCE at 298 K, were plotted at a polarization scan rate of 60 mV/min. Before all experiments, the potential was stabilized at free potential during 30 min. The polarization curves are. In order to investigate the effects of temperature and immersion time on the inhibitor performance, some test were carried out in a temperature range 298–328K. The linear Tafel segments of anodic and cathodic curves were extrapolated to corrosion potential to obtain corrosion current densities (I_{cor}). Measurements were performed in the 1.0 M HCl. The inhibition efficiencies (%) for potentiodynamic polarisation measurements were calculated as follows:

$$EI_{Icor}\,(\%) = \frac{I^{0}_{cor} - I_{cor}}{I^{0}_{cor}} \times 100 \qquad (1)$$

where I_{cor} and I_{cor}^{0} are the corrosion current densities in the absence and the presence of the inhibitor.

2.2.2. Electrochemical impedance spectroscopy

The electrochemical impedance spectroscopy (EIS) measurements was carried out with a same equipment was used as for the polarization measurements, leaving the frequency response analyser out of consideration. After the determination of steady-state current at a corrosion potential, sine wave voltage (10 mV) peak to peak, at frequencies between 100 kHz and 10 mHz were superimposed on the rest potential. Computer programs automatically controlled the measurements performed at rest potential after 30 min of exposure. All potentials were reported versus saturated calomel electrode (SCE). The impedance diagrams are given in the Nyquist representation. Experiments are repeated three times to ensure the reproducibility. The best semicircle can be fit through the data points in the Nyquist plot using a non-linear least square fit so as to give the intersections with the x-axis. The percentage inhibition efficiency (%) in the case of impedance measurements were calculated as follows, where R_t and R_t^0 are the charge transfer resistance values without and with inhibitor, respectively.

$$EI_{Rt}(\%) = \frac{R_t - R_t^0}{R_t} \times 100 \qquad (2)$$

2.3. Computational chemistry

All quantum theoretical calculations were performed with Gaussian03, E.01 software package [17] for PC using density function theory (DFT) 6-31G(d,p) basis set at B3LYP (The Becke's Three Parameter Hybrid Functional using the Lee-Yang-Parr) level [18], starting without any geometry constraints for full geometry optimizations. The following quantum chemical indices were considered: the energy of the highest occupied molecular orbital (E_{HOMO}), the energy of the lowest unoccupied molecular orbital (E_{LUMO}), $\Delta E = E_{HOMO} - E_{LUMO}$ and the dipole moment (μ).

According to Koopman's theorem [19] the ionization potential (IE) and electron affinity (EA) of the inhibitors are calculated using the following equations.

$$IE = -E_{HOMO} \qquad (3)$$

$$EA = -E_{LUMO} \qquad (4)$$

Thus, the values of the electronegativity (χ) and the chemical hardness (η) according to Pearson, operational and approximate definitions can be evaluated using the following relations [20]:

$$\chi = \frac{IE + EA}{2} \qquad (5)$$

$$\eta = \frac{IE - EA}{2} \qquad (6)$$

The number of transferred electrons (ΔN) was also calculated depending on the quantum chemical method [21-22] by using the equation:

$$\Delta N = \frac{\chi_{Fe} - \chi_{inh}}{2(\eta_{Fe} + \eta_{inh})} \qquad (7)$$

Where χ_{Fe} and χ_{inh} denote the absolute electronegativity of iron and inhibitor molecule η_{Fe} and η_{inh} denote the absolute hardness of iron and the inhibitor molecule respectively. In this study, we use the theoretical value of χ_{Fe} =7.0 eV mol^{-1} and η_{Fe} = 0 eV mol^{-1}, for calculating the number of electron transferred.

3. Results and Discussion

3.1 Concentration effect

3.1.1. Gravimetric result

Weight loss measurements of steel were investigated in 1M HCl in the absence and presence of various concentrations of inhibitor at 6 h of immersion and 298 K. The inhibitory efficiency (Ew%) of 4-methyl-2,3-dihydro-1H-1,5-benzodiazepin-2-one (**MDBO**) is calculated as follows:

$$E_W(\%) = 1 - \frac{W'_{corr}}{W_{corr}} \times 100 \qquad (8)$$

Where W_{corr} and W'_{corr} are the corrosion rate of C38 steel in 1M HCl in absence and presence of inhibitor, respectively. The analysis of these results Table 2 shows clearly that the corrosion rate decreases W_{corr} while the inhibition efficiency Ew% increases with increasing inhibitor concentration reaching a maximum value of 89.00 % at concentration of 10^{-3} mol /L. This result reveals clearly that the compound investigated is efficient inhibitor against carbon steel dissolution in 1.0 M HCl solution. The inhibition of corrosion of carbon steel by **MDBO** can be explained in terms of adsorption of inhibitor molecules on the metal surface [23-24].

Table 2: Weight loss data of carbon steel in 1.0 M HCl for various concentration of the 4-methyl-2,3-dihydro-1H-1,5-benzodiazepin-2-one (**MDBO**).

Inhibitor	**Concentration mol/L**	**W_{corr} (mg. cm^{-2})**	**E_w (%)**
Blank	1.0	1.204	-
MDBO	10^{-3}	0.132	89.00
	10^{-4}	0.181	84.93
	10^{-5}	0.267	77.76
	10^{-6}	0.342	71.52

3.1.2. Polarization curve results

The potentiodynamic polarization curve for C38 steel in 1 M HCl solution at 298 K and in the absence and the presence of **MDBO** at various concentrations are exposed in Fig. 2. It can be seen that the tested organic compound caused a decrease in both anodic and cathodic current densities. This shows that the addition of **MDBO** reduces metallic dissolution and consequently retards the hydrogen evolution reaction [25-26]. In addition of inhibitor, the cathodic current–potential curves give rise to parallel Tafel lines, which indicate that hydrogen evolution reaction is activation controlled and that the addition of the **MDBO** does not modify the mechanism of this process [27]. Electrochemical corrosion kinetics parameters such as corrosion current density (I_{cor}) obtained by extrapolation of Tafel lines, corrosion potential (E_{cor}) and cathodic Tafel slope (β_c), together with inhibitor efficiency EI_{Icor} (%) are assumed in Table 3. An inhibitor can be classified as cathodic or anodic if the displacement of potential corrosion value is less than 85 mV, the inhibitor can be seen as mixed type [28-29]. In our investigation, the maximum displacement in E_{cor} value was 23mV for **MDBO** which indicates that the inhibitor acts as mixed type inhibitor with predominant cathodic.

The I_{cor} value decrease with addition of **MDBO** inhibitor in corrosive medium and reached a minimum value at 10^{-3} M corresponding to the greater values of inhibition efficiency. This may be attributed to the adsorption of inhibitors over the corroded electrode surface which confirms the inhibitive action of the **MDBO** toward acid corrosion of steel [30]

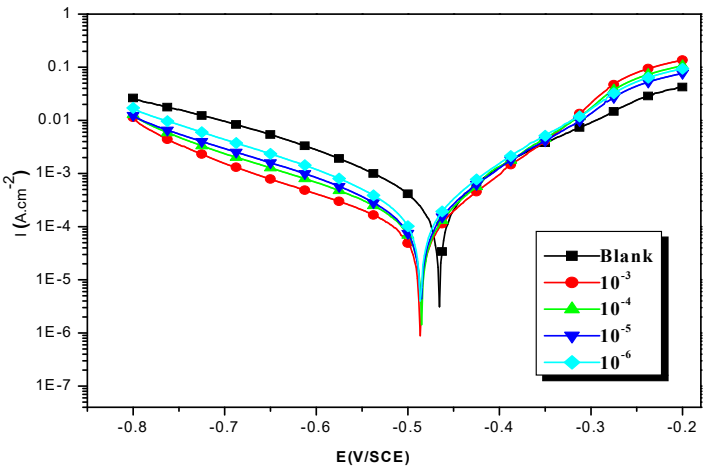

Figure 2: Potentiodynamic polarization curves of C38 steel in 1M HCl in the presence of different concentrations of **MDBO**

Table 3: Electrochemical parameters of C38 steel at various concentrations of **MDBO** in 1M HCl and corresponding inhibition efficiency.

Inhibitor	Conc (M)	$-E_{cor}$ (mV/SCE)	$-\beta_c$ (mV dec^{-1})	I_{cor} (µA cm^{-2})	EI_{Icor} (%)
Blank	1.0	463	168	636	--
MDBO	10^{-3}	486	178	82	87.11
	10^{-4}	484	173	103	83.80
	10^{-5}	486	175	158	75.16
	10^{-6}	486	174	197	69.02

3.1.3. Electrochemical impedance spectroscopy measurements

Corrosion and inhibition behavior of tested material in acidic solution with different concentrations of the experienced inhibitor and its blank solution after immersion for 30 min was studied by EIS at room temperature. Fig. 3 shows the Nyquist plot obtained at the open circuit potential after immersion for 30 min for different concentrations (10^{-3} - 10^{-6}M). The Nyquist plots detected for uninhibited and inhibited solution present a single the capacitive loop which characterize that the process of dissolution metal was mainly controlled by charge transfer. These loops show imperfect semi-circles owing to the phenomenon of dispersing effect which can be related to the roughness and inhomogeneity of the solid surfaces and adsorption of inhibitors [31]. The Nyquist plots were analyzed with Zview 2 software by fitting the experimental data to a simple equivalent circuit model [32]. The fitted parameters including; the solution resistance R_s, the charge transfer resistance (R_{ct}) and the constant phase element (CPE) are tabulated in Table 4. The value of double layer capacitance (C_{dl}) may be determined using the following equation:

$$C_{dl} = \sqrt[n]{Q.R_{ct}^{1-n}} \qquad (9)$$

Where Q are the constant phase element (CPE) and n are a coefficient can be used as a measure of surface inhomogeneity. For n = 0, the constant phase element represents a resistance, for the ideal electrodes, if n = 1 the constant phase element are an ideal capacitance and for n = 0.5 a Warburg element.

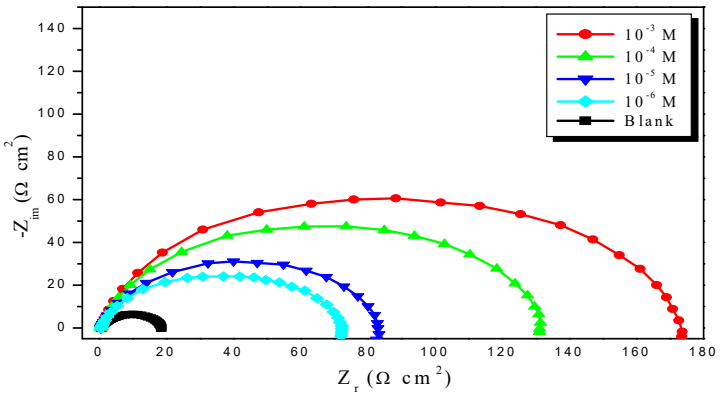

Figure 3 : Nyquist diagrams for C38 steel electrode with and without **MDBO** at E_{corr} after 30 min of immersion.

Table 4. Electrochemical Impedance parameters for corrosion of steel in acid medium at various contents of **MDBO**

Inhibitor	C (mol/L)	R_{ct} ($\Omega.cm^2$)	C_{dl}($\mu F/cm^2$)	E_{RT} (%)
Blank	1.0	18	221.16	
MDBO	10^{-3}	172	37.03	89.53
	10^{-4}	128	49.76	85.94
	10^{-5}	82	77.675	78.05
	10^{-6}	65	97.99	72.31

Examination of EIS result, the charge-transfer resistance value R_{ct} increased with increasing inhibitor concentration, indicating that the recovery of the metal surface is performed by the adsorption of organic molecules. The diminution of C_{dl} with rises of inhibitor concentration, this behavior can be due to a rise in the thickness of the double layer and/or a diminution in local dielectric constant, this variation explained the inhibitor molecule function by adsorption at electrode/solution interface [33]. These suggestions based to the following relation [34]:

$$C_{dl} = \frac{\varepsilon\varepsilon_0}{\delta} S \qquad (10)$$

Where δ is the thickness of the protective layer, S is the surface of the used electrode, ε_0 is the permittivity of the air and ε is the dielectric constant of medium. We can conclude thus, the EIS result confirms that obtained by the potentiodynamic polarization and gravimetric measurements.

3.2 Temperature Effect

The investigation of temperature effect is very important seen your their impact on dissolution process in interface electrode-medium. The corrosion behavior of carbon steel in acidic solution at different temperatures was studied by EIS method in the presence of 10^{-3}M inhibitor and absence of inhibitor (Figure 4). The temperature impacts on the electrochemical parameters of carbon steel are, in the absence and presence of **MDBO**, listed in Table 5. It is clear from Table 5 that the rise of oxidization rate is more pronounced with the augmentation of temperature for uninhibited solution. The presence of the **MDBO** leads to a decrease in the corrosion rate. The inhibitory action of tested compound remains unchangeable with the variation of the temperature from 298 to 328 K. This behaviour led to the conclusion that a protective film of tested molecules formed on the carbon steel surface is thermally stable.

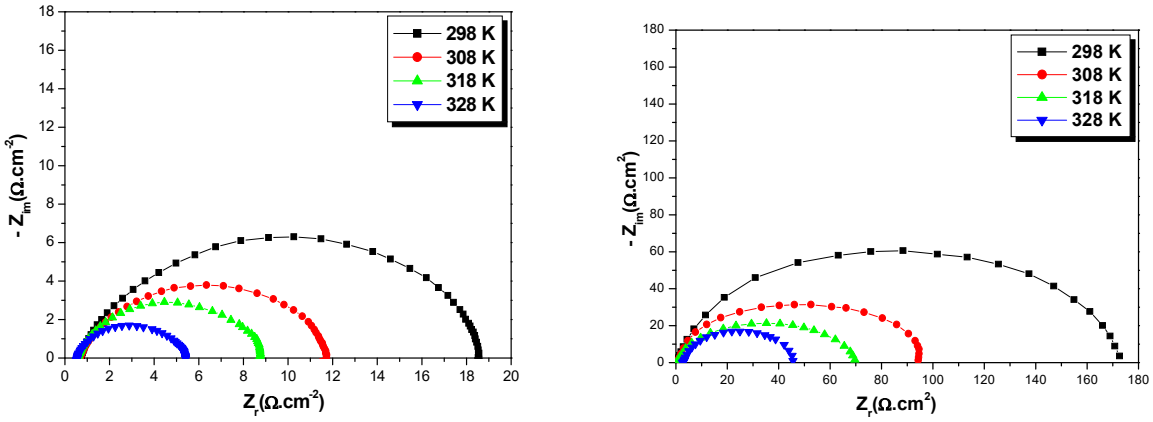

Figure 4: Nyquist plots for corrosion of steel in 1M HCL at different temperature

Table 5. Temperature effect on the carbon steel corrosion in free acid and **at 10^{-3} mol/L of MDBO.**

Inhibitor	Temp (K)	R_{ct} ($\Omega.cm^2$)	C_{dl} ($\mu F/cm^2$)	E_{Rct} (%)
Blank	298	18	221.16	--
	308	11	229.78	--
	318	8	199.04	--
	328	5	201.56	--
MDBO	298	172	37.03	89.53
	308	96	41.46	88.54
	318	71	56.06	88.73
	328	45	88.46	88.87

3.3 Thermodynamic activation parameters

The dependence of dissolution speed at temperature can be pronounced by Arrhenius equation and transition state equation:

$$\log I_{cor} = -\frac{E_a}{2.303RT} + A \qquad (11)$$

$$I_{cor} = \frac{RT}{Nh}.\exp(\frac{\Delta S_a}{R}).\exp(-\frac{\Delta H_a}{RT}) \qquad (12)$$

Where: E_a; Apparent activation energy, A; Arrhenius factor, R; Perfect gas constant, T; Absolute temperature, N :Avogadro's number, h :Plank's constant, ΔS_a : Entropy of activation and ΔH_a: Enthalpy of activation.

The linear regression between ln (I_{cor}) and 1/T exposed in Fig. 5 for carbon steel/HCl solution and inhibited by **MDBO** (10^{-3}M), we permitted to subtract the activation energy in the presence and absence of **MDBO** inhibitor and the result is registered in Table 6. The obtained value of E_a in the presence of the **MDBO** is higher than obtained for uninhibited medium. Some researches correlate this raising of Ea value with that the increased thickness of the double layer, which enhances the activation energy of the corrosion process [35]. The activation parameters (ΔHa and ΔSa) for carbon steel corrosion in 1M HCl in the absence and presence of 10^{-3} mol/L of **MDBO** evaluated from the slope (ΔHa/R) and the an intercept of (ln(R/Nh) + (ΔSa/R)) of the plots of ln(I_{cor}/T) against 1/T (Fig. 6) are exposed in Table 6. The positive signs of ΔH_a reflect the endothermic nature of the carbon steel dissolution process suggesting that its

dissolution is slowed [36-37] in the presence of MDBO. The negative values of entropies, obtained for uninhibited and inhibited systems, imply that the activated complex in the rate determining step represents an association rather than a dissociation step, meaning that a decrease in disordering takes place on going from reactants to the activated complex [38]. The thermodynamic reaction between the Ea and ΔH_a cited in Table 6 is verified.

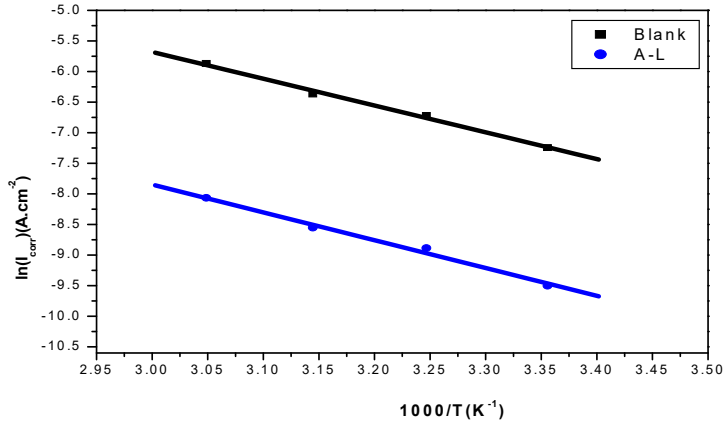

Figure 5: Arrhenius plots of carbon steel in 1.0 M HCl with and without **10^{-3} mol/L of MDBO**

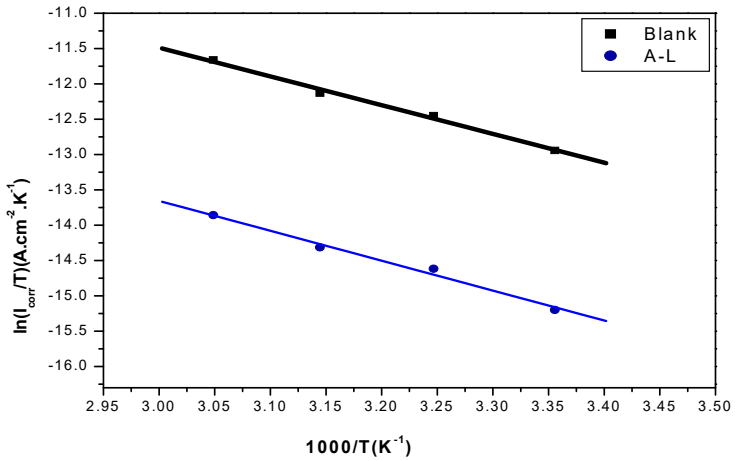

Figure 6: Relation between ln(I/T) and 1000/T in acid at different temperatures in the absence and presence of **of MDBO**

..

Table 6. The value of activation parameters for steel electrode in 1M HCl in the absence and presence of 10^{-3} mol/L of **MDBO**.

Inhibitor	**ΔHa(kJ/mol)**	**ΔSa(J/mol)**	**Ea (kJ/mol)**	**Ea-ΔHa**
1 M HCl	33.79	-191.53	36.38	2.60
MDBO	35.16	-205.41	37.76	2.58

3.4. Adsorption isotherm

The thermodynamic information of inhibitor molecules and carbon steel surface can be delivered by adsorption isotherm [39]. There are several adsorption isotherms such as Langmuir, Temkin, Bockris–Swinkels, Flory–Huggins and Frumkin [40]. The adsorption type can be determined via thermodynamic result gotten from isotherms.

Adsorption of inhibitor molecules at the interface electrode/solution can be explained through substitution of them with water molecules on the metal surface [41]:

$$Org_{(sol)} + xH_2O_{(ads)} \rightarrow Org_{(ads)} + xH_2O_{(sol)} \quad (13)$$

Where $Org_{(sol)}$ and $Org_{(ads)}$ are organic molecules dissolved in medium and adsorbed on electrode surface, respectively. Also, $H_2O_{(ads)}$ is adsorbed water molecule on electrode surface, $H_2O_{(sol)}$ is water molecule in solution and x is size ratio which represents the number of water molecules changed with those of organic compound. Langmuir Isotherm is an appropriate model which is generally used for inhibitor study (Fig. 7). According to this model, the surface coverage (θ) has related to inhibitor concentration (C_{inh}) by the following relation [42-43]:

$$\frac{C_{inh}}{\theta} = \frac{1}{k_{ads}} + C_{inh} \quad (14)$$

Where k_{ads} are the equilibrium constant of the adsorption process. The equilibrium constant for adsorption process is related to the free energy of adsorption, ΔG^0_{ads}, and is expressed by following equation:

$$\Delta G^0_{ads} = -RTln(k_{ads} * 55.5) \quad (15)$$

The thermodynamics parameters derived from Langmuir adsorption isotherms for the investigated inhibitor, are assumed in Table 7. The negative values of ΔG^0_{ads} along with the high k_{ads} designate a spontaneous adsorption process [44]. Generally, the energy values of 20 kJ.mol^{-1} or less negative are related with physisorption between charge of inhibitor molecules and charge of electrode surface, while those around 40 kJ mol^{-1} or higher are binded with chemisorption resulting of the sharing or transfer of electrons from tested molecules to the electrode surface to form a coordinate type of metal bonds [43]. The obtained value of ΔG^0_{ads} suggested that the adsorption of the studied molecules are chemisorption type.

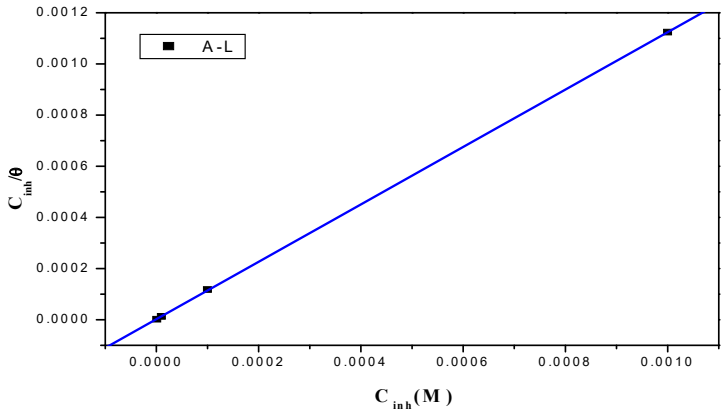

Figure 7 : Langmuir isotherm plots for MDBO adsorption on carbon steel in 1.0 M HCl.

Table.7: Thermodynamic parameters for the adsorption of **MDBO** in 1.0 M HCl on the carbon steel at 298K.

Inhibitor	Slope	k_{ads} (M^{-1})	R^2	ΔG°_{ads} (kJ/mol)
MDBO	1.12	425000	0.99	-42.039

3.5. Quantum chemical calculations

DFT founded quantum chemical calculations were executed on **MDBO** to discovery more insight about the chemical reactivity of the inhibitor molecules. The optimized molecular structures and frontier molecular electron distribution pictures of **MDBO** are shown in Figs. 8. The structure parameters and adsorptive performance of the studied

compound are used to elucidate the inhibition mechanism in the present paper. Various common indices of Quantum chemical such as: energy of highest molecular orbital (E_{HOMO}), lowest unoccupied molecular orbital (E_{LUMO}), energy band gap (ΔE), and fraction of electron transfer (ΔN) are denoted in Table 8. In general, a higher value of E_{HOMO}, is associated with high electron donating ability while, lower value of E_{LUMO} is associated with strong interactions between the molecules inhibitor and electrode surface and therefore a higher value of E_{HOMO} and/ or a lower value of E_{LUMO} is consistent with high electron donating ability and thereby high inhibition efficiency.

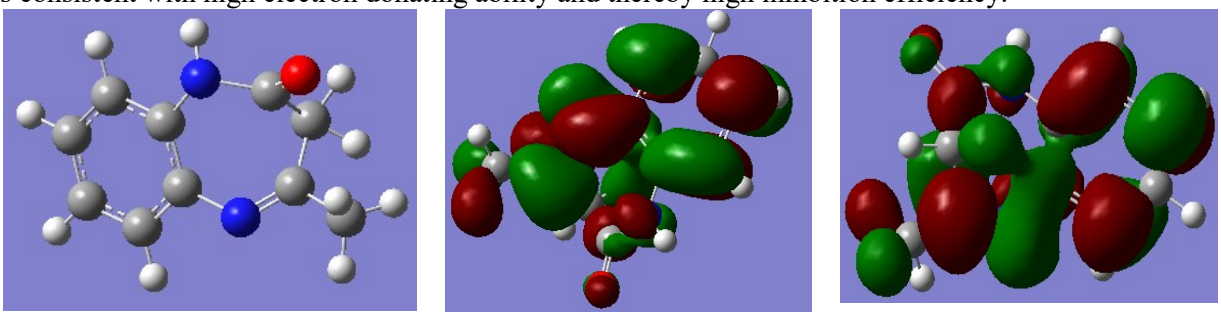

optimized molecular structures HOMO LUMO

Figure 8. The optimized molecular structures HOMO and LUMO of the non-protonated inhibitor molecules using DFT/B3LYP/6-31G (d,p).

Table 8. Calculated Quantum Chemical Parameters of the inhibitor molecules

Propriety	**Value**
Total energy E_T, eV	-571,800
dipole moment **μ, D**	2,5947
E_{HOMO}, eV	-0,23285
E_{LUMO}, eV	-0,04868
energy band gap **ΔE, eV**	0,18417
Ionization potential (IP), eV	0,23285
Electron affinity (EA), eV	0,04868
Chemical potential (χ),eV	0,140765
Global hardness (η), eV	0,092085
Global softness (σ), eV^{-1}	10,85953
fraction of electrons transferred (ΔN)	25,407151

Analysis of Fig.8 shows that the distribution of two energies HOMO and LUMO localized on the double bonds carried by the two rings and the nitrogen and oxygen as heteroatoms, consequently this is the preferred sites for interaction with the electrode surface and the inhibitor molecules. These results propose that the heteroatoms are the probable reactive sites for adsorption of tested molecules on the electrode surface. Higher energy E_{HOMO} of the adsorbent leads to higher electron donating ability [45-46]. Low energy E_{LUMO} designates that the acceptor accepts electrons easily. The highest HOMO energy value of this molecule implied its capability of donating electrons to metallic atoms of electrode, and it has the best inhibitive property. Therefore, the theoretical parameters E_{HOMO} can be used to predicate the inhibition efficiencies of the inhibitors. The energy gap is an important parameter to study. The smaller is the value of ΔE, the more probable it is that the molecule has inhibition efficiencies [47]. The small value of energy gap suggests that the strongest ability of the synthesized inhibitor to form coordinate bonds with d-orbitals of metal

through donating and accepting electrons. The value of the dipole moment μ is higher, which is will favor the improvement of corrosion inhibition. These results are in good agreement with the experimental results obtained. The synthesized inhibitor is donor of electrons and the steel surface is the acceptor, and this favors chemical adsorption of the inhibitor on the electrode surface forming adsorption layer against corrosion. The tested inhibitor shows the highest inhibition efficiency because it has the highest HOMO energy and this reflects the greatest ability of offering electrons. It's clear, from Table 8 that the ability of the synthesized inhibitor to donate electrons to the metal surface, which is in good agreement with the higher inhibition efficiency obtained experimentally. The total energy value obtained indicating that **MDBO** is favorably adsorbed through the active centers of adsorption.

Conclusion

The effect of **MDBO** on the corrosion and inhibition of steel alloy is studied using chemical and electrochemical measurements. The principle conclusions are:

- **MDBO** is originating to be operative inhibitor for steel alloy corrosion in 1.0 M HCl medium.
- Polarization curves show that this compound is of mixed type inhibitor.
- The rise of the **MDBO** concentration leads to a huge diminution of the corrosion current density and the inhibition efficiency is constant with the increase of temperature.
- EIS results showing that the dissolution reaction of steel is controlled by charge transfer process.
- The HOMO and LUMO orbitals show that the favored active sites for an electronic attack and the desired sites for interaction with the electrode surface are located in the area around the nitrogen belonging to the **MDBO.**

References

[1] N. K. Sebbar, H. Elmsellem, M. Ellouz, S. Lahmidi, A.L. Essaghouani, E. M. Essassi, M. Ramdani, A. Aouniti, B. El Mahi and B. Hammouti, Der Pharma Chemica, 7(10) (2015) 9-587.

[2] M. Ellouz, N. K. Sebbar, H. Elmsellem, H. Steli, I. Fichtali, M. M. Mohamed Abdelahi, K. Al Mamari, E. M. Essassi, I. Abdel-Rahaman. J. Mater. Environ. Sci. (2016).7(8), 2806-2819.

[3] K. Bouayad, Y. Kandri Rodi, H. Elmsellem, E. H. El Ghadraoui, Y. Ouzidan, I.Abdel-Rahman, H.S. Kusuma, I. Warad, J.T. Mague, E.M. Essassi and B. Hammouti, A. Chetouani. Mor. J. Chem. 6 (2018) 22 - 34.

[4] P.B .Raja , M.G. Sethuraman , Mater. Corros. 60 (2009) 22–28.

[5] Mamari, H. Elmsellem, N. K. Sebbar, A. Elyoussfi, H. Steli, M. Ellouz, Y. Ouzidan, A. Nadeem, E. M. Essassi and F. El-Hajjaji. *J. Mater. Environ. Sci.* (2016).*7(9), 3286-3299.*

[6] S.A. Abd El-Maksoud , A.S .Fouda , Mater. Chem. Phys. 93 (2005) 84–90.

[7] S.M.A. Hosseini , A. Azim., Mater. Corros. 59 (2008) 41–45.

[8] H .Keles , M .Keles , I.Dehri, O .Serindag, Colloids Surf. A Physicochem. Eng. Aspects. 320 (2008) 138–145.

[9] S.A.Umoren, Li Y., F.H .Wang, Corros. Sci. 52 (2010) 1777–1786.

[10] K.F. Khaled, Electrochim. Acta. 55 (2010) 6523–6532.

[11] R. Alvarez-Bustamante, Electrochim. Acta 54 (2009) 5393–5399.

[12] B.V. Appa Rao, Md.Yakub Iqbal, B.Sreedhar, Electrochim. Acta 55 (2010) 620–631.

[13] G. Avcı, Mater. Chem. Phys. 112 (2008) 234–238.

[14] G. Avcı, Colloids Surf. A Physicochem. Eng. Aspects 317 (2008) 730–736.

[15] A. Saber, H. Zouihri, E. M. Essassi and S. W. Ng; 4-Methyl-2,3-dihydro-1H-1,5 benzodiazepin-2-one monohydrate; Acta Cryst. (2010). E66, o1408.

[16] K. Dioukhane, Y. Aouine, H. Faraj, A. Alami, E. M. Essassi and H. Zouihri.; IUCrData (2019). 4, x181718.

[17] MJ Frisch, GW Trucks, HB Schlegel, GE Scuseria, MA Robb, JR Cheeseman Jr.Gaussian03, revision E.01.Walling ford, CT: Gaussian Inc. (2007).
[18] C. Lee, W. Yang, RG. Phys Rev B. 37(1988)785.
[19] R.G. Pearson, Inorg. Chem. 27 (1988) 734.
[20] V.S. Sastri, J.R. Perumareddi, Corrosion (NACE). 53 (1997) 617.
[21] I. Lukovits, E. Kalman, F. Zucchi, Corrosion (NACE). 57 (2001) 3.
[22] S. Xia, M. Qui, L. Yu, F. Lui, Corros. Sci. 50 (2008) 2021.
[23] I. Ahamad, M. A. Quraishi, 2010. Corros. Sci. 52, 651.
[24] S.K. Shukla, M. A. Quraishi, 2009. Corros. Sci. 51, 1007.
[25] A. Y. Musa, A. Bakar Mohamad, A. Amir H. Kadhum, M. Sobri Takriff, L. Tien Tien, Corros. Sci. 53 (2011) 3672–3677
[26] A. Vasconcelos Torres, R. Salgado Amado, C. Faia de Sa, T. Lopez Fernandez ,C. Alberto da Silva Riehl, A. Guedes Torres, E. D'Elia, Corros. Sci. 53 (2011) 2385–2392.
[27] S. Kertit, B. Hammouti, Appl. Surf. Sci. 93 (1996) 59-66.
[28] A. K. Satapathy, G. Gunasekaran, S.C. Sahoo, K. Amit, P.V. Rodrigues, Corros. Sci. 51 (2009) 2848–2856.
[29] I. Ahamad, R. Prasad, M.A. Quraishi, Corros. Sci. 52 (2010) 1474–1475.
[30] El-Etre A Y, Materials Chem & Phys, 108 (2008) 278.
[31] T. Paskossy, J. Electroanal. Chem. 364 (1994) 111.
[32] M. Belkhaouda, L. Bammou, R. Salghi, A. Zarrouk, Eno. E. Ebenso, H. Zarrok, B. Int. J. Electrochem. Sci., 8 (2013) 10987 – 10999.
[33] E. McCafferty, N. Hackerman, J. Electrochem. Soc. 119 (1972) 146.
[34] E.E. Oguzie, Y. Li, F.H. Wang, Electrochim. Acta. 53 (2007) 909.
[35] R. Solmaz, G. Kardas_, M. Çulha, B. Yazıcı, M. Erbil, Electrochim. Acta 53 (2008) 5941.
[36] N.M. Guan, L. Xueming, L. Fei, Mater. Chem. Phys. 86 (2004) 59–68.
[37] M. Ellouz, H. Elmsellem, N. K. Sebbar, H. Steli, K. Al Mamari, A. Nadeem, Y. Ouzidan, E. M. Essassi, I. Abdel-Rahaman, P. Hristov. J. Mater. Environ. Sci. (2016).7(7), 2482-2497.
[38] S. Martinez, I. Stern, Appl. Surf. Sci. 199 (2002) 83.
[39] F. Bentiss, M. Lebrini, M. Lagrenée, Corros. Sci. 47 (2005) 2915–2931.
[40] A. Ghanbari, M.M. Attar, M. Mahdavian, Mater. Chem. Phys. 124 (2010) 1205–1209.
[41] J. Aljourani, K. Raeissi, M.A. Golozar, Corros. Sci. 51 (2009) 1836–1843.
[42] M. Behpour, S.M. Ghoreishi, N. Mohammadi, N. Soltani, M. Salavati-Niasari, Corros. Sci. 52 (2010) 4046–4057.
[43] H. B. Ouici, M. Belkhouda, O. Benali, R. Salghi, L. Bammou, A. Zarrouk, B. Hammouti, Res Chem Intermed 41 (2015) 4617-4634.
[44] M. Scendo, Corros. Sci. 49 (2007) 373.
[45] N. Khalil, Electrochim. Acta 48 (2003) 2635.
[46] I. Lukovits, K. Palfi, E. Kalman, Corros., 53 (1997) 915.
[47] J. Fang, J. Li, J. Mol. Struct. (Theochem) 593 (2002) 179.